RICE UNIVERSITY

An Investigation of a Relaxation Mechanism in $Nd^{3+}:CaF_2$

by

David Bruce Hadaway

A THESIS SUBMITTED
IN PARTIAL FULFILIMENT OF THE
REQUIREMENTS FOR THE DEGREE OF

MASTER OF ARTS

Thesis Director's signature:

Paul L Donoho

Houston, Texas

May 1967

ABSTRACT

An Investigation of a Relaxation

Mechanism in $Nd^{3+}:CaF_2$

David Bruce Hadaway

The spin lattice relaxation time T_1 of $Nd^{3+}:CaF_2$ was calculated from the spin lattice Hamiltonian determined from strain measurements by T. Black.[1] There is a large discrepancy between this calculation and experimental data. It is proposed that this is due to large displacements of the interstitial charge compensating F^- ions in the host lattice. Preliminary results indicate that they have sufficient mobility and can move quickly enough to cause a faster relaxation time than has been calculated.

CONTENTS

I. INTRODUCTION

Paramagnetic resonance has proven to be a useful tool in investigating the properties of solids. In particular it allows us to analyze with great delicacy a particular facet of the energy structure of a solid that would be completely lost in the bulk properties of the material. A famous example is the examination of the feeble nuclear paramagnetism of iron against the enormous background of ferromagnetism. In this case we are examining an impurity ion, neodymium, in a host lattice of calcium fluoride. The resonance observed is that of Zeeman transitions of an unpaired electron in a rare earth subshell. The electron spin and angular momentum interact with the lattice; the change from the free electron properties allows us to determine the symmetry of the crystalline field and more important to analyze the mechanisms for energy exchange with the lattice which determine the "relaxation time" of the spin system.

This work has dealt with verifying a new mechanism which may explain a large discrepancy between theory and experiment in $Nd^{3+}:CaF_2$.

II. BACKGROUND

1. The lattice and g-factors

The calcium fluoride lattice may be considered as a cubic lattice of fluorine atoms with a calcium atom occupying the center of every other cube. The crystals are grown from a melt of calcium fluoride with the proper proportion of neodymium impurity. The neodymium replaces a calcium atom in the lattice and, being trivalent, requires a charge compensating fluorine ion. The positions of this fluorine ion (which determine the symmetry of the crystalline field acting on the impurity atom) are determined by the past history of the crystal, and in the most common case they are in sites of tetragonal (C_{4v}) crystal-field symmetry. Here the F^- ion occupies one of the six nearest neighbor interstitial sites at a distance of $\frac{a}{2} = 2.73\text{Å}$ where a is the lattice constant. The three crystal-field symmetry directions are the three [100] crystallographic directions. This charge-compensating mechanism has been substantiated by investigations of density and lattice constants by x-ray methods[2] ionic conductivity,[3] as well as by the early paramagnetic results of Bleaney et al.[4] and others.[5]

The electron configuration of Nd^{3+} is $4f^3$ with a ground state of $^4I_{9/2}$. In a tetragonal crystalline electric field, this ground state splits into five Kramers doublets.[4] The splitting between the lowest doublet and the first excited doublet is 65 cm^{-1}[6] so at the temperatures at which we are working, only transitions between states of the lowest doublet are observed (figure 1).

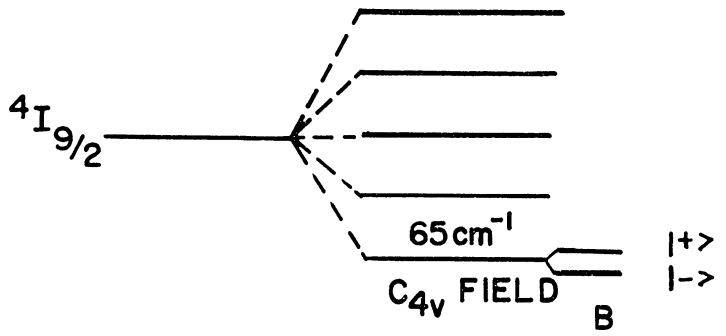

FIGURE 1 ENERGY LEVELS

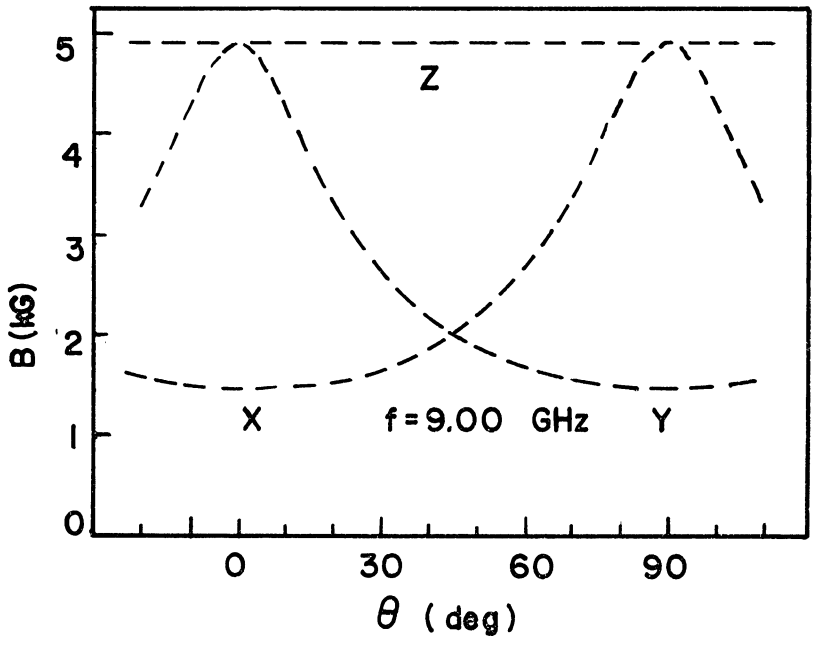

FIGURE 2 LOCUS OF RESONANCE POINTS

The magnetic moment of an electron spin $\vec{\mu}_s$ is

$$\vec{\mu}_s = 2\beta\vec{S}$$

and the magnetic moment associated with the orbital momentum is

$$\vec{\mu}_L = \beta\vec{L}$$

where β is the Bohr magneton $\beta = \frac{e\hbar}{2m}$ and $\vec{S}$ is the spin angular momentum operator and $\vec{L}$ is the orbital angular momentum operator. One may write these equations as

$$\vec{\mu}_s = g\beta\vec{S}$$
$$\vec{\mu}_L = g\beta\vec{L}$$

where g = 2 and 1 for spin and orbital momentum respectively. The g-factor is the ratio of the magnetic moment of the electron to its angular momentum, expressed in dimensionless units by the Bohr magneton. The total magnetic moment is found by vector addition to be

$$\vec{\mu} = g\beta\vec{J}$$

where

$$g = 1 + \frac{J(J+1)+S(S+1)-L(L+1)}{2J(J+1)}$$

for free atoms.

In solids the orbital motion may interact strongly with the crystalline electric fields and become decoupled from the spin, a process called "quenching." The more complete the quenching, the closer the g-value approaches the free electron value of 2.0023. It is found useful to write the magnetic moment in terms of an effective spin alone with an empirical constant $\overleftrightarrow{g}$ which takes into account the anisotropy of the crystalline fields

$$\vec{\mu} = \beta\overleftrightarrow{g}\vec{S}$$

Here, $\overleftrightarrow{g}$ is a symmetric second rank tensor which may be diagonalized, and in our case of axial (tetragonal) symmetry we can write

$$g_{xx} = g_{yy} = g_\perp$$
$$g_{zz} = g_\parallel$$

where $\parallel$ and $\perp$ refer to directions relative to the symmetry axis. The effective spin Hamiltonian is

$$\mathcal{H} = \beta [g_\perp (S_x H_x + S_y H_y) + g_\parallel S_z H_z]$$

For $S = \frac{1}{2}$ we can transform coordinates to obtain[7]

$$\mathcal{H} = E = \pm \tfrac{1}{2} \beta H_0 (g_\parallel^2 \cos^2\theta + g_\perp^2 \sin^2\theta)$$

and the total energy in a transition from + to — is

$$E = g(\theta) \beta H_0$$

where $$g(\theta) = (g_\parallel^2 \cos^2\theta + g_\perp^2 \sin^2\theta)^{\frac{1}{2}}$$

Resonance occurs when $E = \hbar\omega$ where ω is the microwave frequency.

The resonance lines versus field and angle are shown in figure 2 for an ideal $Nd^{3+}:CaF_2$ lattice. Three things should be noted: The line at 5Kg corresponds to the resonance of bonds in the z direction which are always perpendicular to the B field. The high field peak corresponds to $g_\perp = 1.301$ and the low field trough corresponds to $g_\parallel = 4.412$.[6] The high field lines are observed to be stronger than the low field lines.

2. Relaxation Times

Spin-lattice interaction is most commonly analyzed through the phenomenon of spin-lattice relaxation since it is a measure of how easily energy is transferred between the atom and its host lattice. The general case is quite complex as it is a collective result of all interactions of the magnetic system with the lattice. However, at the low temperatures and low concentrations we are considering, the "one phonon" process, associated with the "spin-lattice" Hamiltonian $\mathcal{H}_{SL}$, is dominant. T. D. Black[1] has determined the elements of $\mathcal{H}_{SL}$ using

external stress applied along three axes of the crystal to cause a change in the lattice spacing, and therefore a change in the electric field which determines the g-factors. The change in resonance energy is measured.

The spin lattice relaxation time T_1 is defined for a two level system by the equation

$$\frac{d(\Delta n - \Delta n_0)}{dt} = -\frac{(\Delta n - \Delta n_0)}{T_1}$$

where Δn is the difference in population of the levels, and Δn_0 is the difference in population at equilibrium. The relaxation time is clearly related to the transition probability per unit time W and in fact[7]

$$T_1 = \frac{1}{2W}$$

The total transition probability for the direct (one phonon) interaction is proportional to the squares of the matrix elements of $\mathcal{H}_{SL}$ summed over all phonon modes of frequency $\omega = \frac{\Delta E}{\hbar}$ where ΔE is the energy difference of the two spin levels in question:

$$W \propto \sum |\langle +1 | \mathcal{H}_{SL} | - \rangle|^2$$

P. L. Donoho has carried out the calculation of T_1 on a high speed computer for U^{3+} and Nd^{3+}:CaF_2 and the results are given in figure 3 for Nd^{3+}. Θ is with respect to the z (symmetry) axis and Φ is with respect to the x axis.

A typical calculated value is T_1 = 10 sec at 4.2°K. Bierig et al[8] have measured T_1 in .28% Nd^{3+}:CaF_2 as about 160 μs at the same temperature. Measurements for samples with lower concentrations still gave times less than one millisecond.[9] So there is disagreement between theory and experiment by a factor of at least ten thousand!

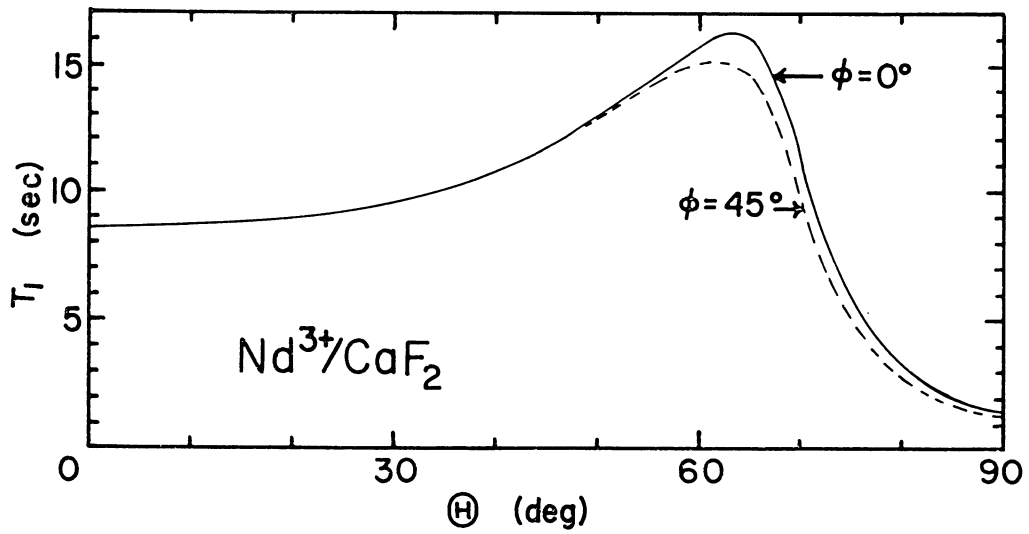

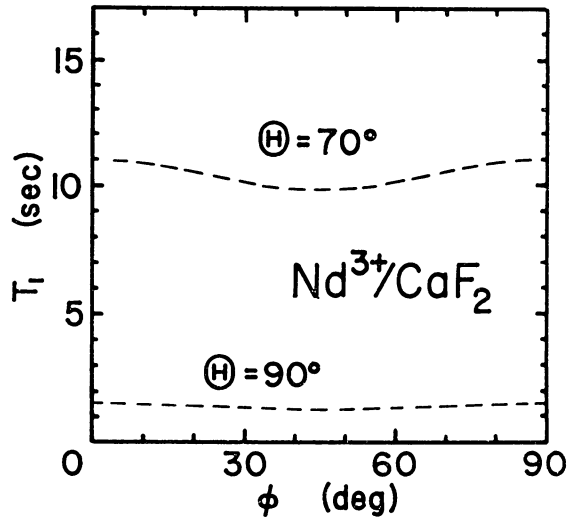

FIGURE 3 CALCULATED RELAXATION TIMES

In all of the strain measurements, the assumption of small displacements was made. Now if the charge compensating F^- ion were able to move to another interstitial site, or alternately, replace one of lattice fluorines which itself then becomes a charge compensating ion, these anomalous results might be explained. If the "jumping" time for the F^- ion were less than the natural relaxation time T_1, then this new mechanism would dominate as far as the system relaxation time.

Watts[9] attempted to investigate this possible mechanism by seeing if saturation of $Nd^{3+}-F^-$ bonds in the z direction had an effect on the resonance of $Nd^{3+}-F^-$ bonds in the y direction. He used a cavity resonant at two different frequencies and chose the magnetic field angle such that the z axis resonance (independent of angle) was at the same magnetic field as the y axis resonance (at the higher frequency). He then saturated (continuously) one of the resonances and inspected the other for some saturation effect due to z bonds becoming y bonds, say. No effect was observed, and he concluded that that mechanism was inoperative. However it could also be concluded that as the F^- ion shifted, it perturbed the Nd^{3+} into relaxing and so introduced no change in the population it was relaxing to.

3. Effect of Electric Field

Since the effectiveness of the suggested mechanism depends on the mobility of the F^- ions at about $4.2°K$ a more direct method of measurement was tried. If an electric field is applied across the crystal, the dipoles formed by the $Nd^{3+}-F^-$ bonds will have energy $\vec{p}\cdot\vec{E}$ which depends on their orientation. Given enough time, the dipoles will orient themselves in the various states in proportions given by Boltzmann statistics--Number $\propto e^{\frac{-p\cdot E}{kT}}$ --since they are all

isolated from each other (low concentration). If the electric field is applied along the x and [100] axis, then precisely six states are available with energies $+pE$, 0 (4-fold degenerate), and $-pE$. The proportion in the lowest energy state is then

$$\frac{e^{\frac{pE}{kT}}}{e^{\frac{pE}{kT}}+e^{\frac{-pE}{kT}}+4}$$

where $E = \frac{V}{d}$

V = voltage applied = 1250V

d = thickness of sample = .86mm

$P = ql = q\frac{a}{2}$

q = charge of ion

a = lattice constant = 2 x 2.73Å

T = 1.6°K

We are considering the electric field on an atomic scale, and do not take into account the polarization charges.[10] The calculated proportions in states of lowest to highest energy are ~ 82%, 18% and .2%. Since the intensity of the resonance line is proportional to the number of neodymium-fluorine pairs contributing to that line, we can calculate the change in intensity due to a change in the distribution from the equilibrium distribution. The purpose of the experiment then is to determine whether and how fast this distribution is attained. Of course, only if it occurs quickly will it be useful in explaining the relaxation times observed.

4. Condition for Resonance

In our experiment we have a static magnetic field $\vec{H}_o$ in the x-y plane and a linearly polarized microwave field in the z direction

(figure 4).

The direction of the microwave field reverses each half cycle. The net field (at the site of the sample) may be represented by two counter-rotating vectors:

$$\vec{H}_{R,L} = H_1 [\hat{i} \cos \pm\omega t + \hat{j} \sin \pm\omega t]$$

where $\vec{H}_{R,L}$ correspond to +w and -w respectively. We will show that one component will induce resonance transitions, and the other will not.

The equation of motion of a magnetic moment in a magnetic field is[11]

$$\frac{d\vec{\mu}}{dt} = \frac{q\beta}{\hbar}(\vec{\mu} \times \vec{H})$$
$$= \frac{q\beta}{\hbar}\vec{\mu} \times (\vec{H}_0 + \vec{H}_1(t))$$

We can eliminate the time dependence of $H_1(t)$ by using coordinates rotating with frequency ω. Then both $\vec{H}_0 + \vec{H}_1(t)$ are stationary and we can write the coordinate transformation as

$$\left(\frac{d\vec{\mu}}{dt}\right)' = \frac{q\beta}{\hbar}\vec{\mu} \times \left[\hat{k}\left(\frac{\pm\omega}{\frac{q\beta}{\hbar}} + H_0\right) + i\frac{q\beta}{\hbar}H_1\right]$$
$$= \frac{q\beta}{\hbar}\vec{\mu} \times H_{effective}$$

The magnetic moment therefore precesses about a static magnetic moment $\vec{H}_{eff}$ (figure 5). Now if the electron were free, this precessing motion would not absorb any energy (except for a "starting transient") but in a real solid, some coupling to the lattice will allow it to dissipate energy (and relax). For the case of $H + \frac{\omega}{\frac{q\beta}{\hbar}}$ the absorption will depend only weakly on the frequency, but for $H - \frac{\omega}{\frac{q\beta}{\hbar}}$, there will be a sharp peak in absorption for $H = \frac{\omega}{\frac{q\beta}{\hbar}}$ corresponding to the case of the electron spin executing violent swings between +z and -z (remaining perpendicular to $\vec{H}_1$).

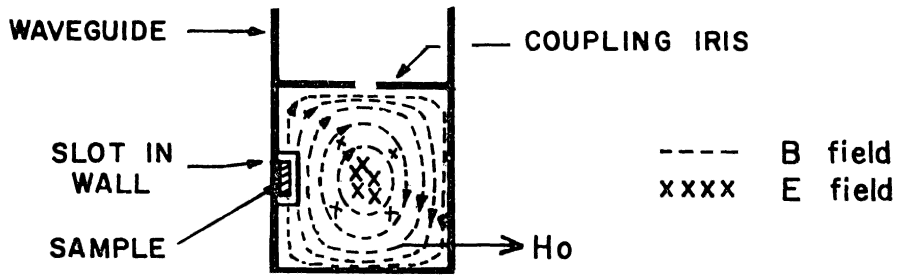

FIGURE 4 FIELDS IN CAVITY

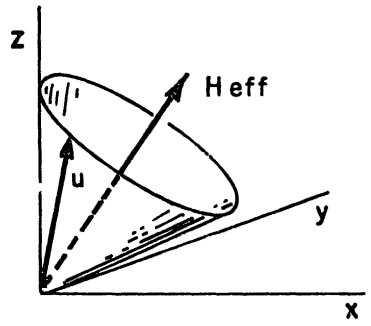

FIGURE 5 PRECESSION IN ROTATING FRAME

III. EXPERIMENTAL APPARATUS

1. Preparation of Samples

The samples were platelets of .07% neodymium doped calcium fluoride cut from a large optical-quality single crystal blank obtained from Harshaw Chemical Company. They were aligned and cut into rectangular slabs (using Laue x-ray equipment and a diamond cutting saw) with the [100] axes perpendicular to the face, and parallel to the edges.

The electric field was to be applied between a silver film plated on the sample face and the cavity wall, with the film being much less than a skin depth in thickness to allow the microwaves to penetrate the sample without being attenuated significantly.

For a plane conductor, the distance δ at which the electric and magnetic fields have decreased to $\frac{1}{e}$ of their surface values is

$$\delta = \frac{1}{\sqrt{\pi f \mu \sigma}}$$

where μ is the permeability (= 1 for nonmagnetic materials) and σ the conductivity. If we wish the attenuation to be less than 10% then the thickness is $.1\,\delta$ = 700 Å for silver at room temperature with a frequency of 9 gHz.

Initially the vacuum plating was done using simple geometrical considerations to determine the film thickness resulting from a known amount of metal evaporated in a molybdenum trough. When it became apparent that the films were still so thick as to seriously perturb the microwave field (drastically lowering the "Q" of the cavity), a "minimum thickness" film was deposited by monitoring the resistance of a reference plate during evaporation.

Films obtained in this way had a resistance across the long dimension of the platelet of $\sim 5\Omega$, corresponding to a calculated thickness of 30 Å. Unfortunately, silver is deposited in granular layers at thicknesses less than 100 Å,[12] so this film perhaps was probably thicker, but non-uniform. It would be pointless to plate thinner films and hope for reliable conductivity across the sample.

These films were still unsuitable for an experiment, since a silver plated cavity with a Q of ~ 2000, exhibited a Q of 100 when the plated sample was placed on the inside wall. With such a low Q, the microwave magnetic field which induces the resonance transitions would be smaller than normal (B is proportional to $Q^{\frac{1}{2}}$), and the method of stabilizing the klystron via a correction signal obtained from the curvature of the cavity resonance curve would be quite insensitive to small changes in frequency because of the low curvature of a low Q resonance.

The problem was finally solved by the use of high resistance paints (designed for printed circuit resistors) made by Micro-Circuits Company. These are available in six resistance ranges covering the range from 30 ohms to 25 megohms. The very high resistance paint was finally used, giving a ten megohm resistance across the sample. The electrical connection was a flattened wire epoxied to the end, with silver paint making good contact to the resistive film. Insulating lacquer was applied over the entire surface to reduce electrical breakdown over the edges. Breakdown essentially ceased below a helium pressure of 10 mm Hg.

2. Mechanical Equipment

The sample cavity was a silver plated section of copper wave guide with brass endplate operating in the TE_{101} mode ($\frac{1}{2}$ guide wavelength long at 9 gHz). The maximum RF magnetic field is parallel and adjacent to the narrow wall of the cavity and reverses direction each half cycle. A slot was cut in the cavity to allow the sample to be pressed flat against the narrow wall (held by vacuum grease) and to protrude outside for the high voltage connection.

Because the Q of the cavity depended strongly on the resistance of the film (which changed with temperature) as well as how far the sample was inserted into the cavity, it was found necessary to use a variable coupling mechanism. To digress briefly, the coupling is a measure of how much power is reflected, and how much is "absorbed" by a cavity. If the power is principally reflected from the iris then the coupling coefficient β is less than unity, and the cavity is "undercoupled." If the power is principally reflected from the rear of the cavity, β is greater than unity and the cavity is overcoupled. When the reflections cancel, all power is absorbed by the cavity, $\beta = 1$ and the cavity is "unity coupled." Clearly it is desirable to be near unity coupling to allow the sustaining of large standing waves in the cavity, creating large microwave fields to influence the sample.*

The variable coupler consisted of a teflon wedge moving in a section of waveguide narrowed below cutoff immediately before the cavity. The dimensions used were as follows (figure 6):

*From theory, the maximum sensitivity is obtained slightly off unity.[13]

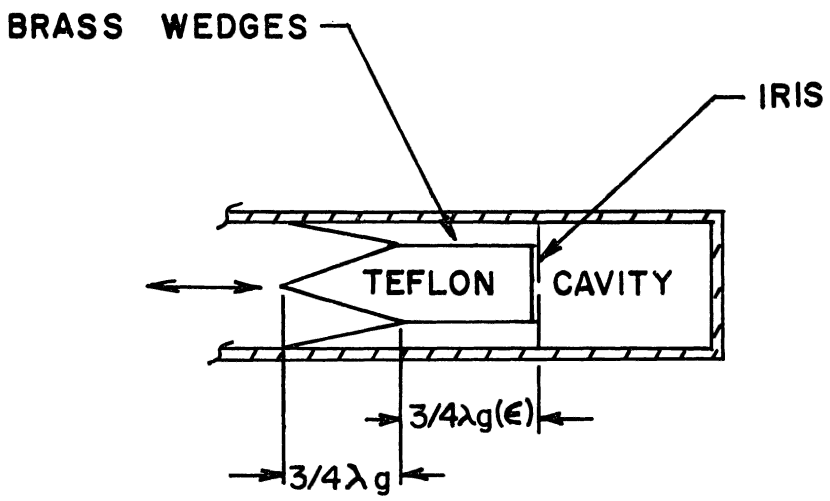

FIGURE 6 REMOTE COUPLING DEVICE

$$\lambda_g = \frac{\lambda_f}{\sqrt{1 - \frac{\lambda_f}{\lambda_c}}}$$

$$\lambda_{g(\epsilon)} = \frac{\lambda_f}{\sqrt{\epsilon_r - \frac{\lambda_f}{\lambda_c}}}$$

λ_g = guide wavelength

$\lambda_{g(\epsilon)}$ = guide wavelength in Teflon

λ_f = free space wavelength at cavity resonance

λ_c = free space wavelength at cutoff = $2a$

a = broad dimension of waveguide

ϵ_r = relative dielectric const.

The iris is selected for slight overcoupling at room temperature. The waveguide should be narrowed until

$$\lambda_c = \frac{\lambda_f}{c}$$

where c is an empirical constant > 1 and ≈ 1.25.

The electrical lead was #40 copper wire enclosed in a teflon tube with stainless steel outer jacket for shielding.

3. Spectrometer

Initial runs were made with a conventional spectrometer (figure 7) using field modulation and phase sensitive detection. However the EPR signals from the $Nd^{3+}:CaF_2$ were only marginally above the noise, and not very reproducible. Then a superheterodyne system was set up with stabilization to an external cavity which gave good signals but had the disadvantage that any drift of the sample cavity resonant frequency would cause a dispersive (frequency dependent)

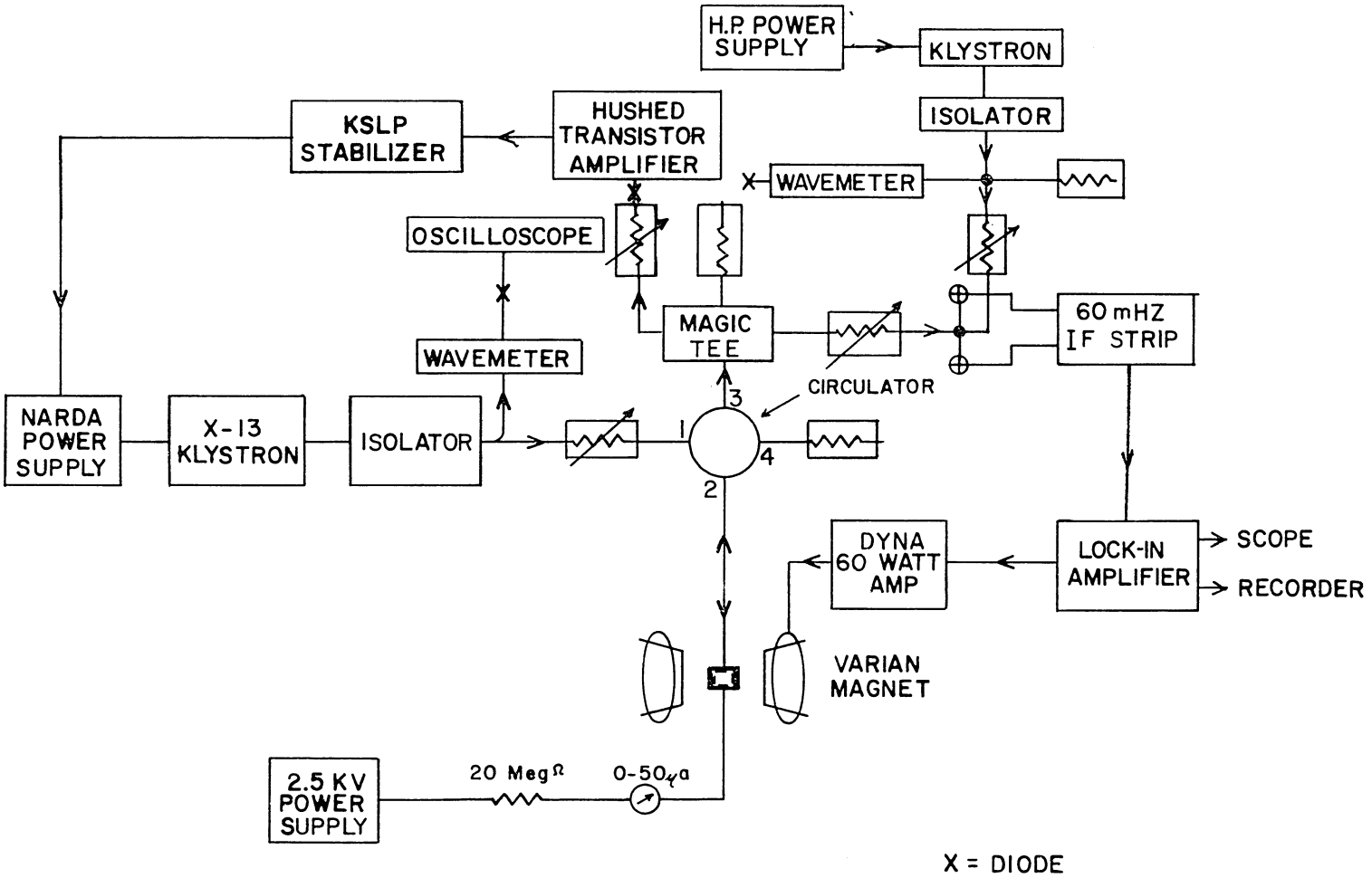

FIGURE 7 SUPERHETERODYNE SPECTROMETER.

component in the signal. The final system used stabilization to the sample cavity, with some difficulties due to the low power levels used in a typical superheterodyne system to avoid saturation.

The klystron stabilizer kept the klystron on the cavity resonant frequency by injecting a 70 kHz modulation into the reflector voltage (and thus the frequency), then detecting the 70 kHz signal reflected from the cavity (zero on resonance) to provide a correction to the reflector voltage to bring the klystron back to the center of the resonance dip of the cavity. The magnetic field was modulated by an audio amplifier driven by the reference oscillator in the lock-in amplifier, and for a field modulation small in comparison with the EPR absorption dip, an amplitude modulated signal will be generated that is proportional to the slope (derivative) of the EPR signal. The power reflecting from the cavity was split by a magic tee. Part went to a diode detector, low-noise transistor pre-amplifier and to the stabilizer. The preamp was used to reduce the noise resulting from the low power levels--20 db gain was satisfactory (more gain tended to overload the stabilizer input). The rest went to the balanced diode mixer where it was mixed with the power from a reference klystron tuned 60 mHz apart in frequency. The reference klystron was not stabilized, but stayed within the 2 mHz bandwidth of the IF strip after a few hours warm-up. The mixer operation relies on the non linear properties of the diode: for small voltages, the current is

$$i = a_1 v + a_2 v^2 + \cdots$$

where the second term is the only one contributing to rectification. If v is the sum of two sine waves of different frequencies, a simple

expansion shows that there is a term corresponding to a difference frequency which contains all the modulation information in the original signals. (Balanced diodes were used to cancel out klystron noise). The IF strip is a high gain tuned amplifier which rejects all noise outside its frequency range from 59 to 61 mHz. The output was detected by a diode, and was finally phase-sensitive-detected by the lock-in amplifier at the same frequency as the field modulation. The lock-in uses a tuned AC amplifier with a Q of 25, then chops and synchronously rectifies the output at the reference frequency, then applies DC amplification and filtering (if necessary) to give a DC signal proportional to the input times the sine of the relative phase angle. The general principle is that it is easy to find something if you know where (and when) to look for it. Here we know the frequency and the phase, and can thus recover signals far <u>below</u> the noise.

IV. EXPERIMENTAL PROCEDURE

The sample was placed against the wall of the cavity with vacuum grease, the electrical lead attached and a small amount of DPPH included for a reference signal (Diphenyl picryl hydrazyl has an unpaired electron whose g-factor approaches the free electron value). The system was checked at liquid nitrogen temperature, helium liquid was transferred, and after a second check then the helium was pumped on to reach a temperature of about 1.6 °K. The cavity was adjusted to unity coupling. The main klystron was tuned, then locked to the cavity resonant requency. The local oscillator klystron was first tuned 60 mHz different from that frequency, and then tuned to the center of the IF strip bandwidth by observing the 70 kHz output of the IF strip (coming from the stabilizer).

The klystron stabilizer did not fully stabilize the klystron (because of the low power used) so it was found necessary to correct the reflector voltage for minimum jitter and noise in the IF strip output. This condition did not always correspond to zero correction voltage (perhaps due to asymmetry in the cavity resonance dip).

V. RESULTS AND CONCLUSIONS

The preliminary work was to plot the EPR spectrum of $ND^{3+}:CaF_2$ versus field and angle. It became evident that this was not in fact a perfect crystal since the spectrum was slightly asymmetrical. However the line peaks agreed with the published g-values for the crystal, so no great importance was attached to this.

For the main measurement, the magnetic field and angle were adjusted until we were on the high field resonance peak (corresponding to neodymium-fluorine "y-axis" bonds perpendicular to the magnetic field: $g_\perp$), we trimmed the field until the lock-in showed the maximum derivative, then applied the electric field parallel to the magnetic field. The signal immediately dropped in amplitude; and when the field was removed, it immediately rose again. The rise and fall time was faster than the response of the chart recorder. The changes were reproducible over short intervals, but prolonged application of the field caused a change in the peak amplitude of the signal.

The immediate change in amplitude could be attributed to several mechanisms: Perhaps the ions were shifting a small amount, causing the resonance to appear at a different magnetic field value, and thus causing an <u>apparent</u> change in amplitude. This was checked by changing the magnetic field and, in fact, we were still on the maximum of the resonance line. Also, the neodymium fluorine bonds may have changed in orientation, causing the resonance to appear at a different angle for the given field. A change of more than a few degrees would take us completely off the resonance line, yet for small displacements one would then expect that the change would increase with applied electric

field. But increasing the field from 1250V to 2000V had little or no effect on the amplitude of the change. Also, a magnetic field sweep showed no shift or change in the resonance line except for its amplitude. The remaining mechanism is that of large displacements of the interstitial fluorine atoms, causing a change in the populations in the six tetragonal positions about the neodymium.

The two charts show the effect of an electric field on the high field line corresponding to bonds in the x- or y- axis. The first chart (figure 8) is a plot of $\frac{d\chi''}{dB}$ versus B for $B \perp E$ with the x-axis being driven by the Hall effect gaussmeter to eliminate hysteresis. Using our previous calculation, we would expect a shift in "population" from 4.9 to 2 when the field is turned off. The observed change is about 15% less than this. The second chart (figure 9) is a plot of the maximum of $\frac{d\chi''}{dB}$ versus time for $B \parallel E$. Here we would expect a change from 2 to 1.1 when the field is turned on. The observed changes vary around this value. A definite tendency was noticed for the changes to decrease during the course of a run. Further work should be done with a sample that has been heated to randomize the bond orientations. Starting from this initial state we can then observe the effect of electric field and temperature.

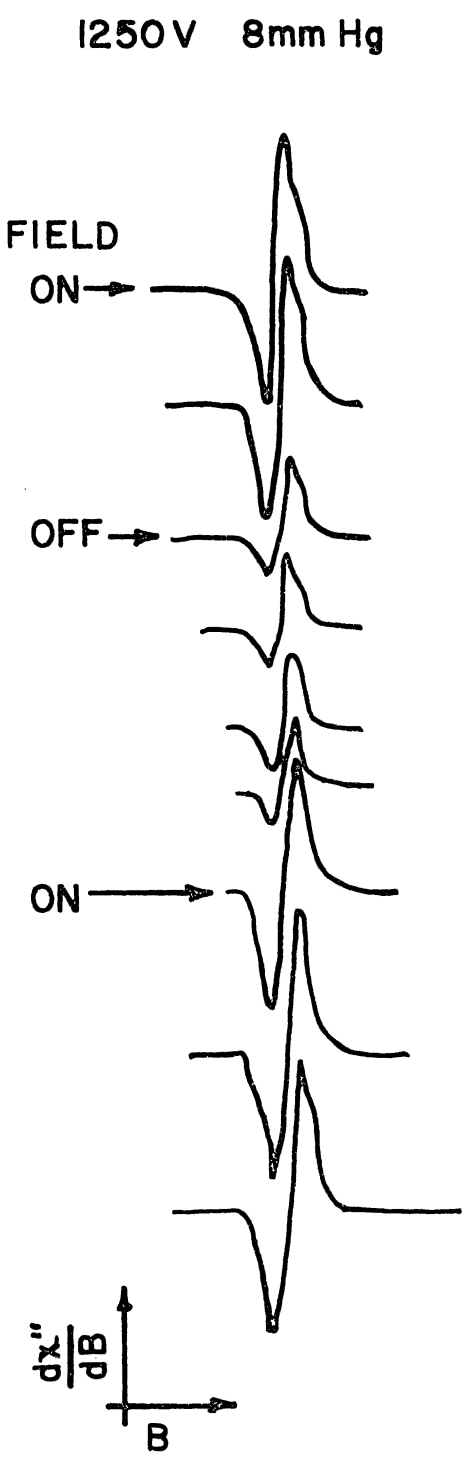

FIGURE 8 ABSORPTION DERIVATIVE VS. FIELD FOR B⊥E

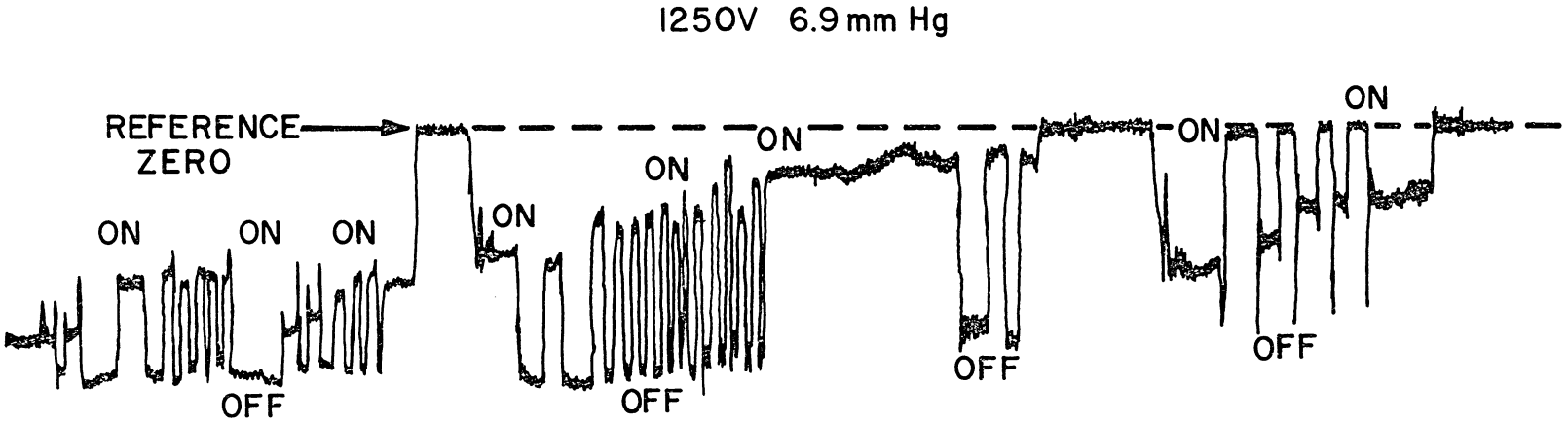

FIGURE 9 MAXIMUM ABSORPTION DERIVATIVE VS. TIME FOR BIIE

REFERENCES

1. T. D. Black, Ph.D. Thesis, Department of Physics, Rice University, 1964 (unpublished).

2. R. W. M. D'Eye and F. S. Martin, J. Chem. Soc. 349, 1847 (1957).

3. R. W. Ure, J. Chem. Phys. 26, 1363 (1957).

4. B. Bleaney, P. M. Llewellyn, and D. A. Jones, Proc. Phys. Soc. (London) B69, 858 (1956).

5. J. M. Baker, W. Hayes, and M. C. M. O'Brien, Proc. Roy. Soc. (London) A254, 273 (1960).

6. M. J. Weber, R. W. Bierig, Phys. Rev. 134, A1498 (1964).

7. G. E. Pake, Paramagnetic Resonance, New York: Benjamin (1962) pp. 30-39.

8. R. W. Bierig, M. J. Weber, and S. I. Warshaw, Phys. Rev. 134, A1504 (1964).

9. R. K. Watts, Ph.D. Thesis, Department of Physics, Rice University, 1965 (unpublished).

10. Panofsky and Philips, Classical Electricity and Magnetism, Mass.: Addison-Wesley (1962) pp. 33-34.

11. C. P. Slichter, Principles of Magnetic Resonance, New York: Harper and Row (1963) p. 19.

12. L. Holland, Vacuum Deposition of Thin Films, London: Chapman and Hall (1961) p. 241.

13. C. P. Poole, Electron Spin Resonance, New York: Interscience (1967).

ACKNOWLEGEMENTS

I would like to thank Dr. P. L. Donoho who suggested this thesis topic, and H. Blackstead who helped greatly in experimental techniques.